Journal of Naval Sciences and Engineering
2020, Vol. 16, No.1, pp.45-70
Mechanical Engineering/Makine Mühendisliği

RESEARCH ARTICLE

EFFECT OF THE NITRIDING PROCESS IN THE WEAR BEHAVIOUR OF DIN 1.2344 HOT WORK STEEL

Seda ATAŞ BAKDEMİR[1]
Doğuş ÖZKAN [2]
M. Cenk TÜRKÜZ [3]
Elif UZUN[4]
Serdar SALMAN[5]

[1]*National Defence University, Turkish Naval Academy, Mechanical Engineering Department, Istanbul, Turkey,*
sabakdemir@dho.edu.tr; ORCID: 0000-0003-1601-2033

[2]*National Defence University, Turkish Naval Academy, Mechanical Engineering Department, Istanbul, Turkey,*
dozkan@dho.edu.tr; ORCID: 0000-0002-3044-4310

[3]*Titanit Ultra Hard PVD Coatings Company, Istanbul, Turkey,*
cenk.turkuz@titanit.com.tr; ORCID: 0000-0002-4447-7287

[4]*Marmara University, Metallurgical and Materials Engineering Department, Istanbul, Turkey,*
elif.uzun@marmara.edu.tr; ORCID: 0000-0002-4950-2162

[5]*National Defence University, Rectorate of National Defense University, Istanbul, Turkey,*
ssalman@marmara.edu.tr; ORCID: 0000-0002-9184-3876

Date of Receive: 08.03.2020 **Date of Acceptance: 02.04.2020**

Seda ATAŞ BAKDEMİR, Doğuş ÖZKAN, M. Cenk TÜRKÜZ, Elif UZUN, Serdar SALMAN

ABSTRACT

Gas nitriding is a widely applied thermochemical surface treatment, which is applied to enhance mechanical properties and wear characteristics of iron and steels. The impact of the gas nitriding process on the mechanical and wear resistance characteristic of DIN 1.2344 (X40CrMoV5-1) hot work steel were investigated in this paper. Nitrided and non-nitrided samples were characterized through a different method such as the optical microscope, scanning electron microscopy, energy dispersive spectrometry, X-ray diffraction, atomic force microscope (AFM) and 3D optical profilometer. The results of analyses reveal that increases in wear resistance of the nitrided sample due to the formation of surface layers of nitrides and oxides.

Keywords: *Gas Nitriding, Wear Behavior, DIN 1.2344 Steel, Atomic Force Microscope.*

Seda ATAŞ BAKDEMİR, Doğuş ÖZKAN, M. Cenk TÜRKÜZ, Elif UZUN, Serdar SALMAN

NİTRASYON İŞLEMİNİN DIN 1.2344 SICAK İŞ TAKIM ÇELİĞİNİN AŞINMA DAVRANIŞLARI ÜZERİNE ETKİLERİ

ÖZ

Gaz nitrasyon yöntemi demir ve çeliklerin mekaniksel özelliklerini ve aşınma karakteristiklerini geliştirmek için uygulanan bir termokimyasal yüzey işlemidir. Bu çalışmada DIN 1.2344 (X40CrMoV5-1) sıcak iş takım çeliğine uygulanan gaz nitrasyon işleminin mekanik özelliklerine ve aşınma direncine etkisi araştırılmıştır. Nitrürlenmiş numune ve işlem görmemiş referans numune optik mikroskop, SEM EDX, X ışını difraksiyonu, atomik kuvvet mikroskopu ve 3D optik profilometre yoluyla karakterize edilmiştir. Analiz sonuçları nitrürlenmiş numune yüzeyinde oluşan nitrür alaşımları ve oksidasyon tabakası sayesinde aşınma direnci artış meydana geldiğini göstermiştir.

Anahtar Kelimeler: *Gaz Nitrasyon, Aşınma Davranışı, DIN 1.2344 Çeliği, Atomik Kuvvet Mikroskopu.*

1. INTRODUCTION

The success of high technology countries is mostly the result of continuous and efficient running systems in industrial applications. The effective life of system components is an important phenomenon in mechanical systems [1]. In recent years, there has been a growing submission for surface treatments that can alter the surface properties of different materials by developing their physical and chemical characteristics like wear and corrosion resistance, hardness, fatigue strength, coefficient of friction, etc [2]. The nitriding is a famous process for supplying surfaces with better tribological properties [3]. The nitriding process is a thermochemical surface treatment based on the development of the surface with nitride phases in consequence of the diffusion of nitrogen ions into the material surface [4]. The nitriding process is carried out at low temperature as compared with alternative surface hardening techniques such as carburizing and carbonitriding. Hereby the steel stays in the ferrite phase (or cementite depending on the alloy composition) along the process. Quenching is not needed in the nitriding process and thanks to distortions are at the minimum level. Additionally, the nitriding process is comparatively practical to audit by process parameters and core hardness [5].

The formation of the nitrided case results from the “compound layer” and “diffusion zone" from the surface to the core. Two different structures are shown in Figure 1. The field under the diffusion zone is the core of the steel including tempered martensite. The compound layer contains epsilon phase (ε -$Fe_{2\text{–}3}N$), gamma phase (γ-Fe_4N) or a mixed-phase (ε+γ) [6]. Phase structure and thickness of the compound layer notably influence the material's mechanical properties. A longer nitriding time is needed to form γ-Fe_4N whereas ε -$Fe_{2\text{–}3}N$ can easily be formed on the surface and grown over time because the γ-Fe_4N structure that can nucleated and grown within the ε structure [7]. The fact that the white layer consists only of these intermetallic compounds ensures that the hardness is independent of the chemical composition of the material. However, the white layer has an extremely hard and fragile structure. Therefore, it can cause material deformation and crack under contact conditions [8]. Meanwhile, the white layer should be reduced or removed greatly by some methods such as grinding and chemical dissolution from the surface before using the nitrided part. The nitrogen is found as an intermediary atom in the iron cubic or finely dispersed alloy nitride in the diffusion zone. The hardness value decreases due to the decreasing amount of nitrogen in the inner parts of the steel [9]. While the white layer contributes to the development of the corrosive properties, the diffusion layer improves the tribological properties and fatigue strength of the steels [10].

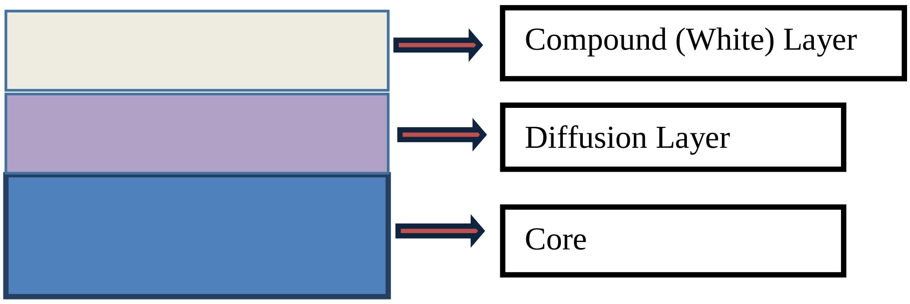

Figure 1. Formation nitrided case [6].

There are three types of nitriding methods: gas, liquid and ion nitriding which Ammonia is used in gas nitriding. Nitrogen decomposes from ammonia gas, reacts with iron and alloy elements in steel and then forms fine-grained nitrides. Liquid nitriding is done in salt baths containing NaCN. Some of the nitrogen and carbon in the cyanide (CN) penetrate the steel. Ion nitriding is based on the ionization and bombardment of a mixture of gases such as nitrogen and hydrogen, on the surface of the material [11].

DIN 1.2344 is widely used in hot die applications, die casting and extrusion dies, wear-resistant tools, high pressure die casting tools and pressing tools. Since DIN 1.2344 hot work steel is exposed to a compeller mechanical and thermal shocks, its wear and corrosion resistance, hardness should be improved through several surface treatments [12]. This study presents the wear and friction behavior of gas nitrided DIN 1.2344 hot work steel. Previous works showed that the wear rate belongs to the thickness of the nitrided layer and hardness, toughness [13]. Wear and friction tests were carried out at three different contact pressures. The effect of plasma nitriding discussed in the light of wear rates of the nitrided sample and bare steel comparison with wear mechanisms evaluation.

Table 1. Chemical composition of the DIN 1.2344 hot work steel [14].

Element	**C**	**Si**	**Cr**	**Mo**	**V**
Wt %	0,40	1,00	5,30	1,40	1,00

2. MATERIALS AND METHODS

2.1. Substrate Preparation

DIN 1.2344 (X40CrMoV5-1) hot work steel substrates (30x30x5mm) were selected as the base material. The chemical composition of DIN 1.2344 hot work steel is shown in Table 1 [14]. Before nitriding processes, the substrate should be subjected to some pretreatments for sufficient hardness [15]. The samples are heat-treated by using the consequent steps: austenitizing at 1030°C for 25 minutes, quenching, and after all double tempering (at 590°C and 600°C for 2 hours to remove the internal stresses in the steel. After the first tempering, the expected impact of rough carbide which has a brittle structure, occurred by the transformation of austenite to tempered martensite is reduced during the second tempering step [16]. Substrates were polished to Rq=19.98 nm quadratic surface roughness (measured with atomic force microscopy (AFM)) with sandpapers and then cleaned with isopropanol for 15 min. by the ultrasonic cleaner.

2.2. Nitriding Process and Characterization

Treatments were realized in a gas nitriding furnace which was preheated to 450 °C where the ambient air consists of ammonia and nitrogen gas mixture. The temperature was set to 530˚C during the active nitriding process [17]. The nitrided samples were grinded and polished after mounting with bakelite mold metallographic examination. Polished samples were etched for about 10-15 seconds with 5% Nital [18]. The thickness and microstructures of nitrided layers were observed by an optical microscope. Average (Ra), root mean square roughness (Rq) of the nitrided sample and bare steel sample were obtained by AFM (Nanosurf Flex AFM-5) topography analysis. Surface structure and chemical composition of the nitrided sample and bare steel sample were investigated via SEM Zeiss Ultra Plus field emission scanning electron microscope) and EDX (Bruker XFlash 5010 EDX detector with 123 eV resolution). To specify the phases in the nitrided specimens, X-ray diffractometry (XRD) by the use of Bruker D8 Advance X-ray diffractometer was performed.

2.3. Tribometer Test Condition and Test Parameters

Tribometer (UTS 10/20) with a ball on the flat reciprocating module device was operated to determine the wear behavior of the samples and to obtain the friction coefficient values.

Table 2. Tribometer test condition and test parameters.

Load [N]	5/10/15
Frequency [Hz]	2
Stroke [mm]	5
Sliding Distance [m]	100
Temperature [°C]	24 °C

Alumina balls with a diameter of 6 mm are used at wear test. According to the parameters given in Table 2, wear tests of nitrided and bare steel samples were performed at 5, 10, and 15N loads.

The maximum Hertzian contact pressure was assessed by eq.(1) (: load, $\mathbf{E}'$: Effective elastic modulus, : diameter of the ball) [19].

$$P_{maks} = \frac{1}{\pi}\left(\frac{6xLxE'^2}{R^2}\right)^{\frac{1}{3}} \tag{1}$$

The observed maximum Hertzian contact pressure of the nitrided sample and bare steel sample were shown in Table 3.

Table 3. Hertzian contact pressure.

	Hertzian Contact Pressure (GPa)	
	DIN 1.2344 Bare Steel	**DIN 1.2344 Nitriding**
5N	1.28	1.35
10N	1.61	1.70
15N	1.84	1.95

2.4. Surface and Tribochemical Analysis

Morphological changes and wear mechanisms formations were observed by optical microscope and AFM analysis. Wear scar surfaces were scanned via force modulation mode by using uncoated silicon nitride (Si_3N_4) rectangular PPP-LFMR cantilever with the spring constant of 0.178 N/m. The surface energy of the samples was carried out force-distance mapping on the surfaces with a 16x16 force curve analysis with SPIP 6.7.8 analysis. Wear volumes of the wear scars were evaluated with scanning of the all wear scar surface by an optical profilometer (Sensofar) and then raw data examined with Mountainspip 8 software. Tribochemical evaluation of the tribofilms and worn surfaces were carried out SEM/EDX.

3. RESULTS AND DISCUSSION

3.1. Characterization of The Nitriding Process

X-ray diffraction pattern of this sample showed that the nitriding layer included mainly of α-Fe that slightly γ and ε nitrides formed after the nitriding process (see Figure 2)[6]. A thin compound layer was detected above the diffusion zone that can be explained by the XRD phase analysis diagram which is similar in both samples. This layer is the brittle white layer formed by iron nitrides and it can be removed from the surface by abrasive methods after nitriding [20].

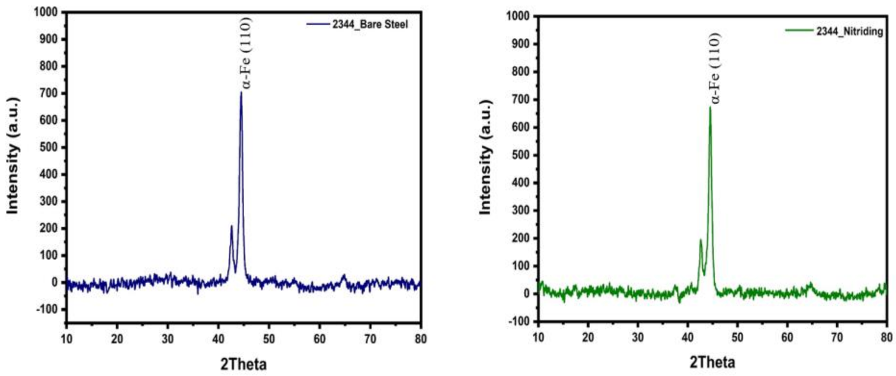

Figure 2. XRD patterns of the 2344 bare steel and 2344 nitrided steel.

The optical microscope, AFM and SEM/EDX images of the samples are shown in Figure 3. AFM topography analysis showed that bare steel and nitrided steel had a different average surface roughness (Ra) and root mean square roughness (Rq), 15.32, 6.64 and 19.98, 8.67 nm, respectively. The decrease in the roughness values of the nitrided surface improved the wear properties. SEM/EDX images showed the nitrogen phase compatibly XRD analysis results. Nitrogen was detected on the nitriding sample surface where the decrease in iron amount indicates the formation of iron nitride structures [21].

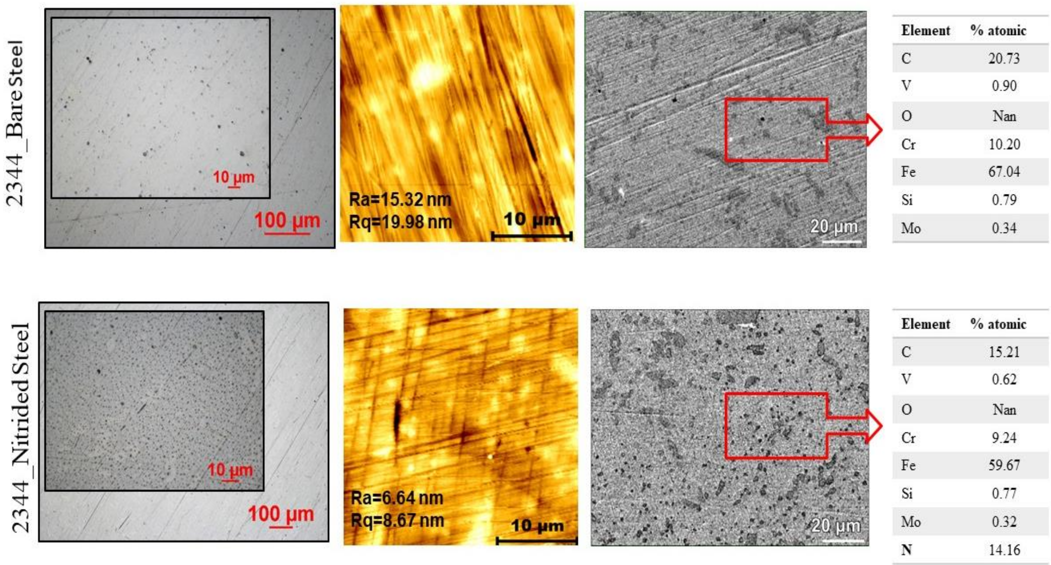

Figure 3. Optical microscope, AFM and SEM/EDX images of the bare steel and nitrided sample.

3.2. Friction Coefficients and Wear Rates

Friction coefficients results are shown in Figure 4. Wear tests are applied at three different loads, the sample that was nitrided under all loading conditions showed a lower friction coefficient. The COFs of 2344 bare steel sample was found to be 1.13, 0.96, 1.15 at 5, 10, 15N, whereas 2344 nitrided steel COFs were 0.58, 0.52, 0.95 at 5, 10, 15N, respectively. The friction coefficient values of 2344 nitrided steel at the 5 and 10 N was approximately 55% lower than the 2344 bare steel. On the other hand, similar COFs were observed at 15N [22]. In addition, the nitriding layer broke down at the sliding distance of 40 m where the COF increase started at 15N.

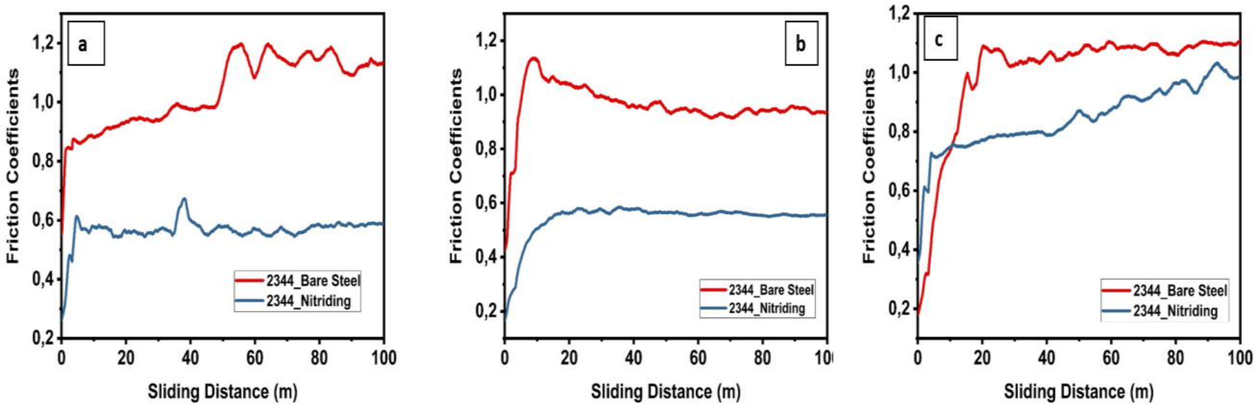

Figure 4. Friction coefficient evaluations (a) COFs at 5 N, (b) COFs at 10 N, (c) COFs at 15 N.

Rockwell C hardness measurement was performed on the sample surfaces under 150 kgf load as shown in Figure 5. The brittle structure on the top of the nitride layer caused cracks in the hardness trace.

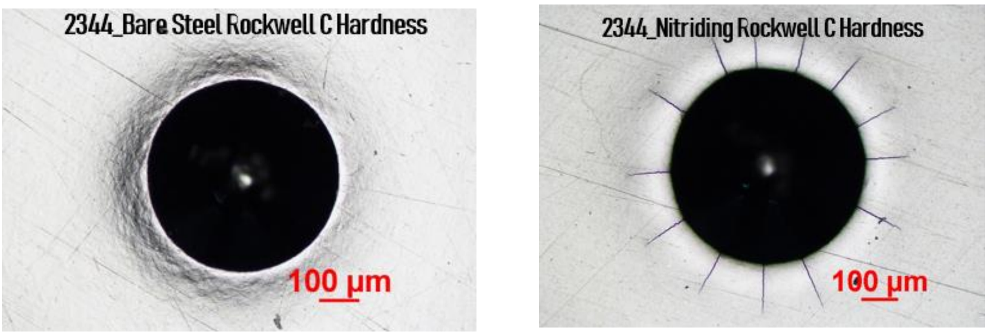

Figure 5. Rockwell C hardness scar of 2344 bare steel and 2344 nitrided steel at 150kgf.

The thickness and microstructures of nitrided and layers were shown in Figure 6. The thickness of the total nitrided layer was measured as 77.99 µm [23].

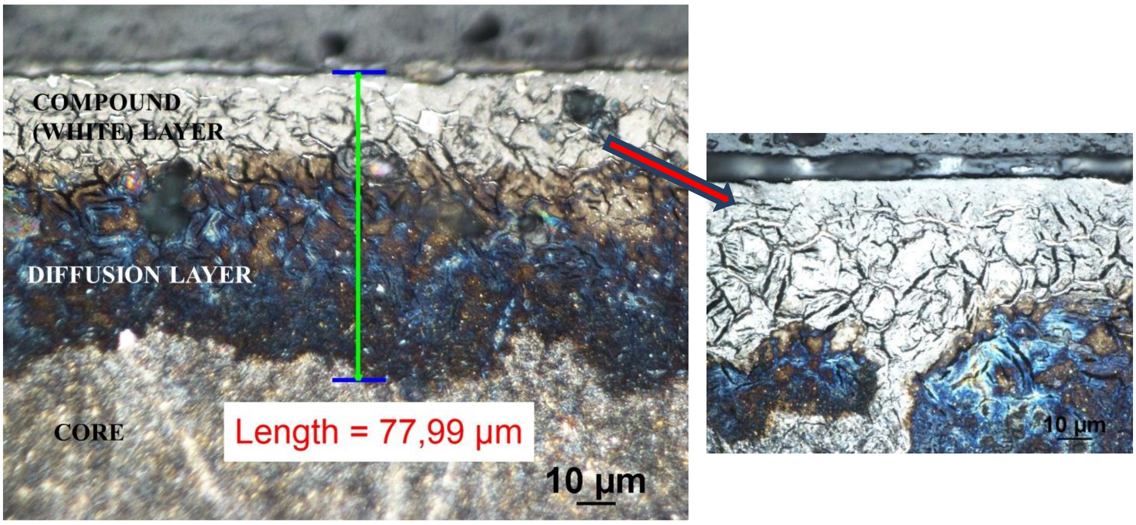

Figure 6. Optical microscope image of the formation nitrided case.

After wear tests, wear line widths of the samples and counter surface images of the alumina ball were obtained with an optical microscope (see Figure 7). The 2344 bare steel sample wear widths were measured to be 425.65, 693.27, 719.72 µm at 5, 10, 15N, respectively and the abrasive wear lines wear homogeneously formed throughout all scars. Wear widths increased with load at the same time, on the other hand, the amount of wear transfer element originated from the counter surface alumina increased with the load. Therefore, the worn area diameter of the alumina ball increases with load. When compared to the wear scar widths of samples, the nitrided sample had approximately 60% lower wear scar width against the bare sample. Abrasive wear lines are not dominant at 5 and 10N, but abrasive wear lines were observed as labeled with yellow arrows at 15N load. The higher wear transfer material was observed on the alumina ball as a result of the high contact pressure at 15N.

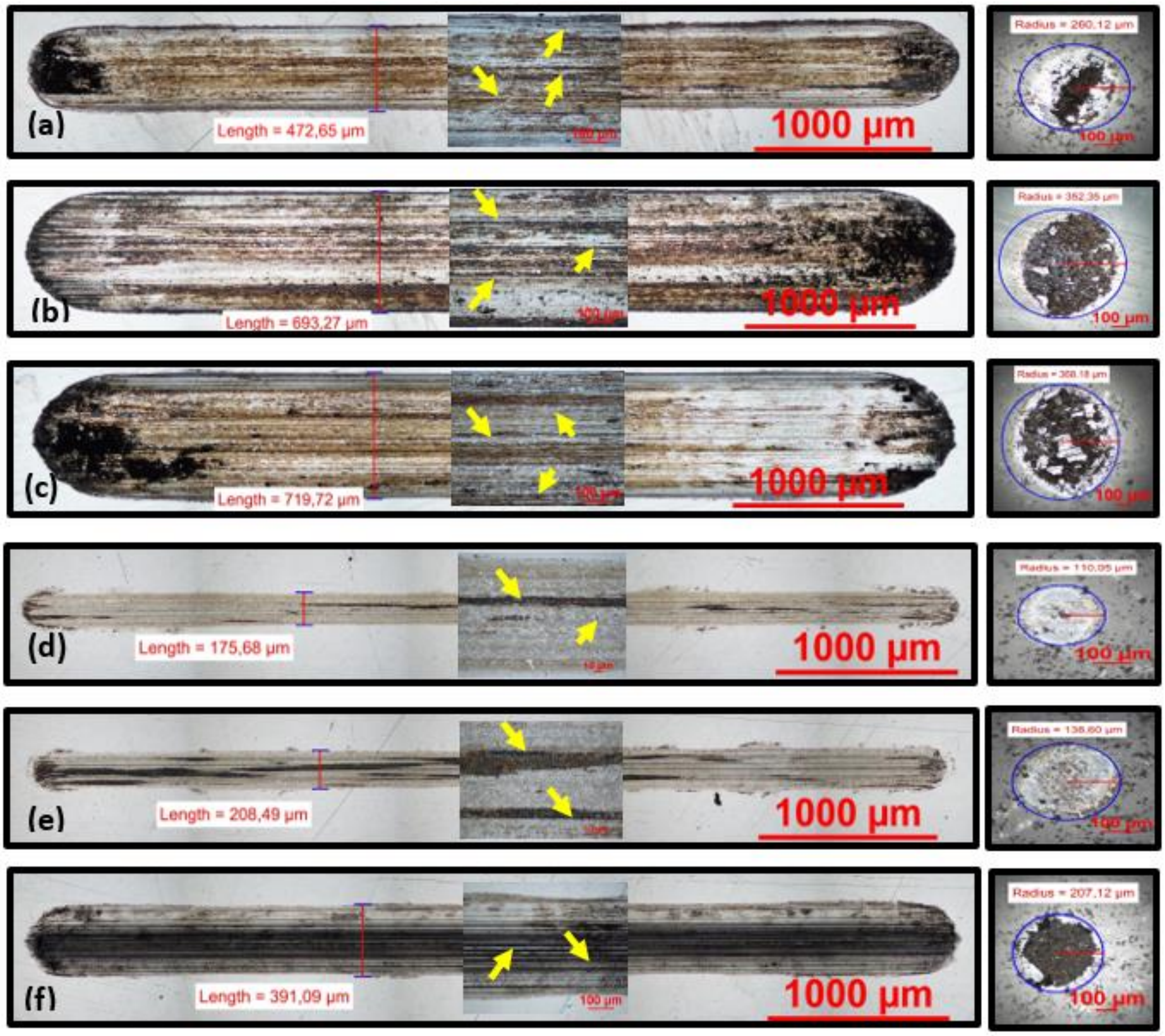

Figure 7. Optical microscope images of the wear scars and alumina ball surfaces, (a), (b), (c) 2344 Bare steel and ball tested at 5,10 and 15N, (d), (e), (f) 2344 Nitrided steel and ball tested at 5,10 and 15N.

The 3D surface profiles of wear scars of nitrided and bare samples tested under a dry sliding condition are shown in Figures 8, 9 and 10. Wear volumes of the wear scars were obtained by scanning all the wear scar surfaces with a confocal optical profilometer.

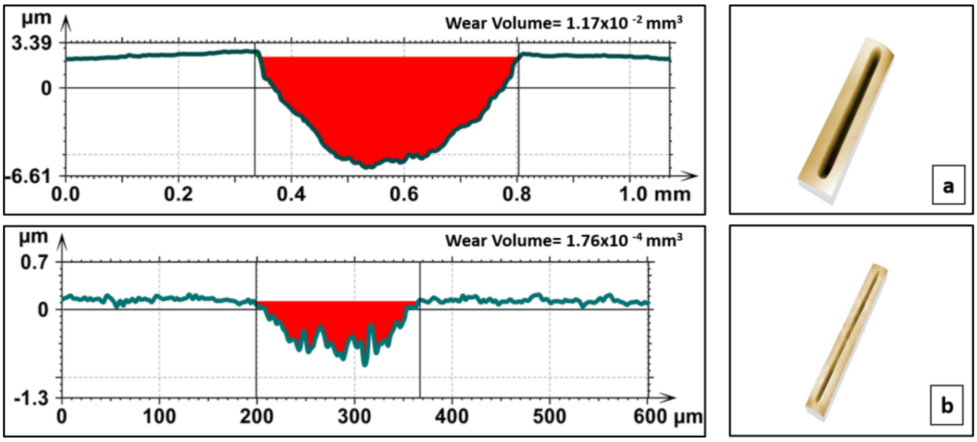

Figure 8. Optical profilometer images of the samples (a) 2344 bare steel and (b) 2344 nitrided steel at 5N.

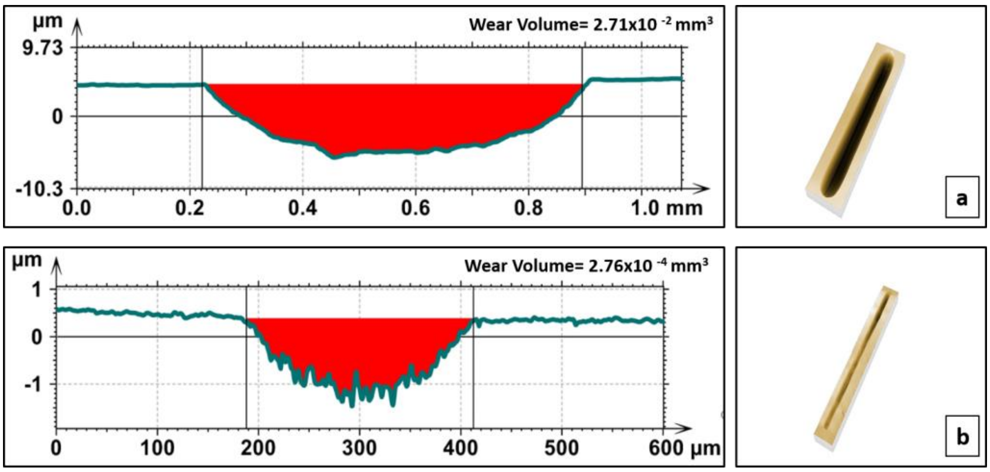

Figure 9. Optical profilometer images of the samples (a) 2344 bare steel and (b) 2344 nitrided steel at 10N.

Mountains map software was used to convert the wear volumes and wear scar cross-sections into numerical values and compare them. When the wear volumes are compared, positive the effect of nitriding can be seen on wear resistance of the bare steel. The wear volumes of nitrided samples were lower than bare steel. This difference in the wear volume of between bare steel and nitriding steel was observed to be approximately 5 times at 1.9 GPa contact pressure (15N).

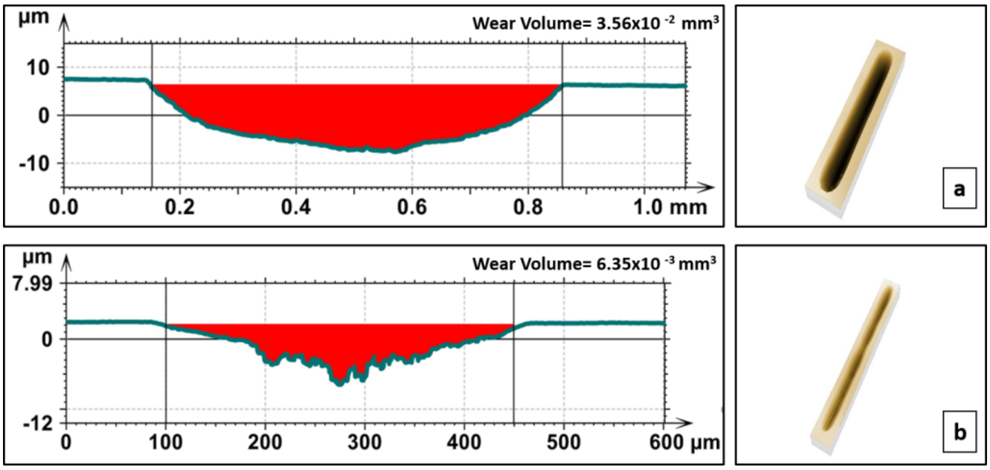

Figure 10. Optical profilometer images of the samples (a) 2344 bare steel and (b) 2344 nitrided steel at 15N.

Wear rates, W_R, were obtained by Archard's equation as shown in Eq. 2 and plotted in Figure 11.

$$W_R = \frac{\Delta V}{F_N \times L} \qquad (2)$$

V (mm^3) is the wear volume, F_N (N) is the applied force and L (m) is the sliding distance at the eq(2) [24].

When looking at the 2344 bare steel sample wear rates were measured to be $2.35x10^{-5}$ mm^3/N.m, $2.71x10^{-5}$ mm^3/N.m, $2.37x10^{-5}$ mm^3/N.m at 5, 10, 15N, respectively and 2344 nitriding sample wear rates were measured to be $3.53x10^{-7}$ mm^3/N.m, $2.76x10^{-7}$ mm^3/N.m, $4.23x10^{-6}$ mm^3/N.m at 5, 10, 15N, respectively. Nitrided 2344 steel showed the best wear resistance with the $2.76x10^{-7}$ mm^3/N.m at 10N [25].

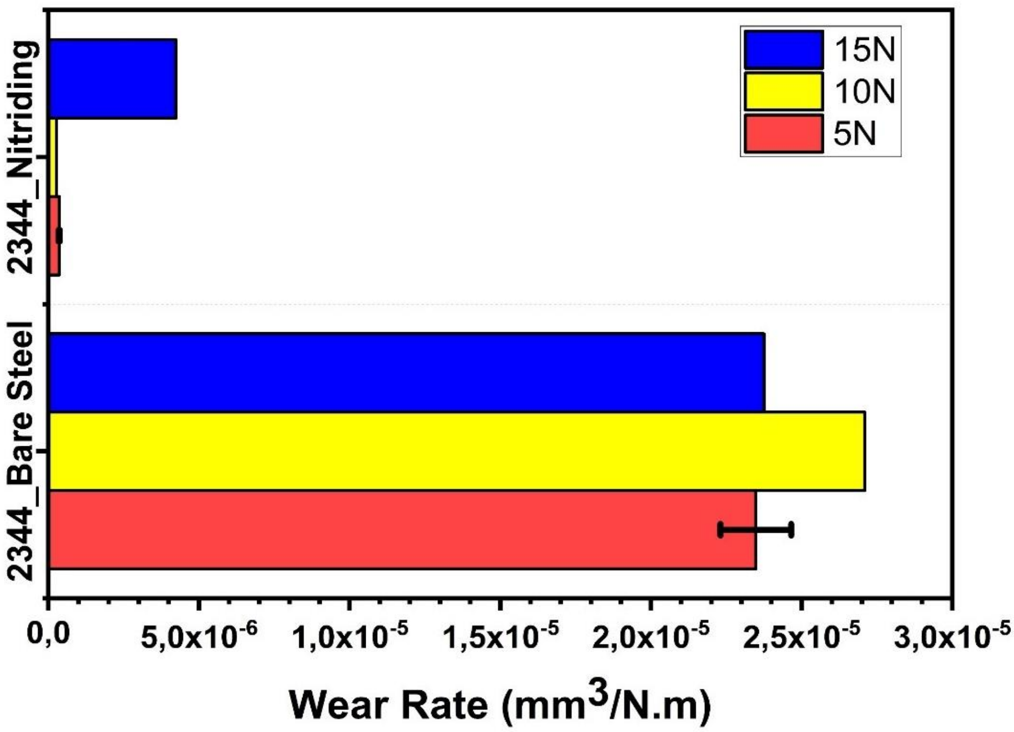

Figure 11. Wear rates of 2344 bare steel and 2344 nitrided steel at 5N, 10N, 15N.

Figure 12 and Figure 13 shows AFM topography analysis of abrasive wear scars of 2344 bare steel and nitride steel, respectively. Abrasive wear scars depths were 373, 614, and 512 nm at 5, 10, and 15N for 2344 bare steel. Abrasive wear scars depths were 238, 485, and 510 nm at 5, 10, and 15N for 2344 nitrided steel [26].

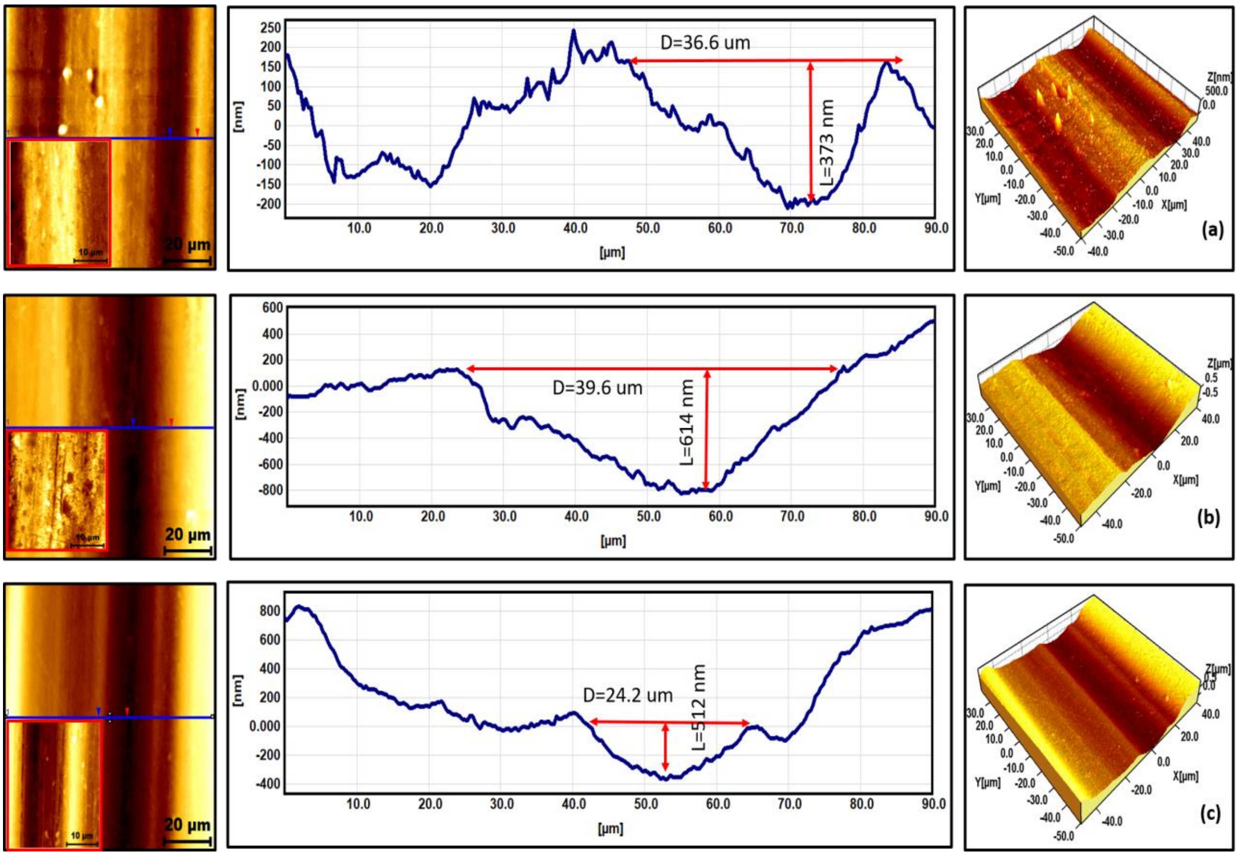

Figure 12. AFM analysis of the wear scars of 2344 bare steel (a) 5N, (b) 10N and (c) 15N.

It can be seen that the application of a higher load scales up the scratch depth. In addition, the nitrided sample has a lower wear scar depth than the bare steel sample. The wear scar depths in 10N and 15N loads have approximately the same values in both samples[27-28].

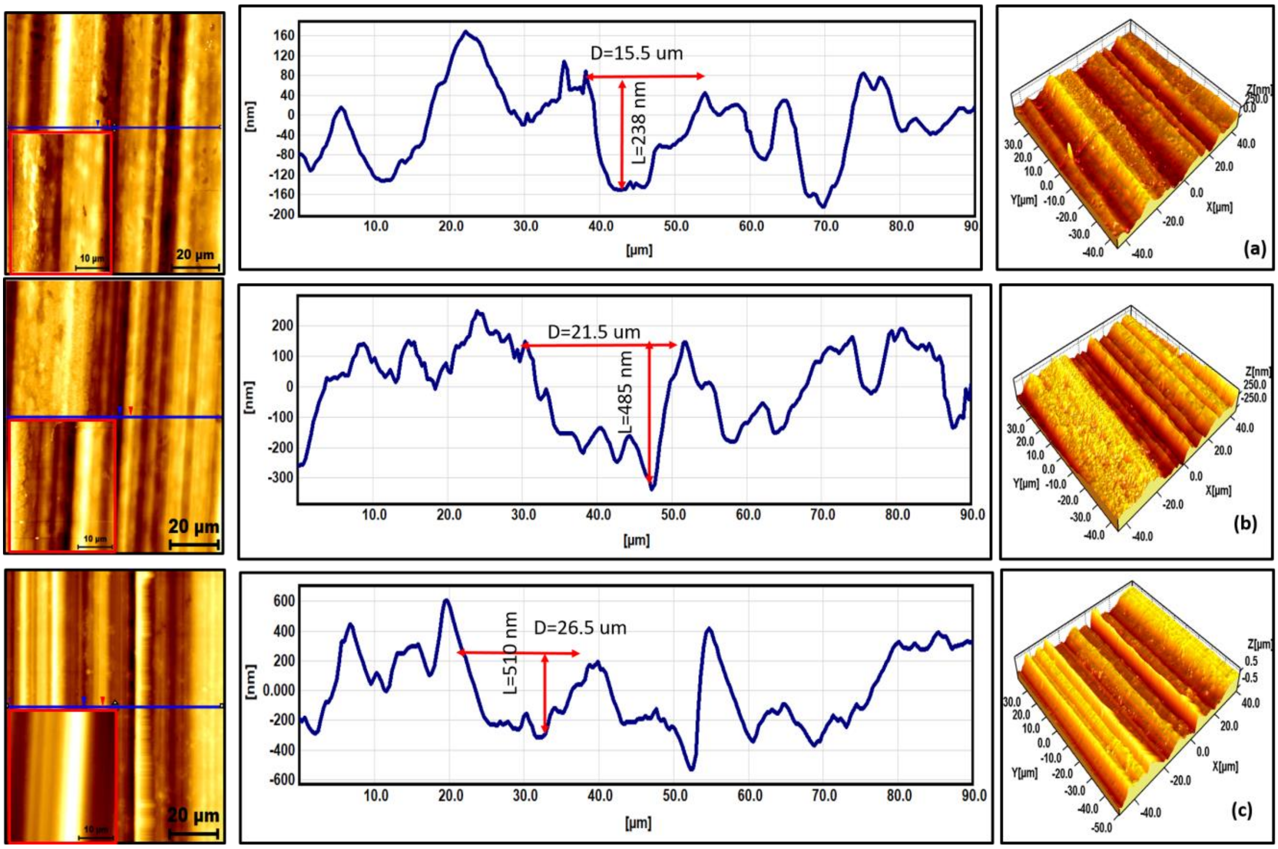

Figure 13. AFM analysis of the wear scars of 2344 nitrided steel (a) 5N, (b) 10N and (c) 15N.

3.3. Tribochemical Analysis of The Worn Surfaces

SEM/EDX results were shown in Figure 14. When the elemental composition of the 2344 bare steel wear scars is examined, the elements that constitute the chemical composition of 2344 steel and oxygen are determined. The reason for this is the oxide layer formed on the surface as a result of contact of the wearing surface with air during the wear test [10].

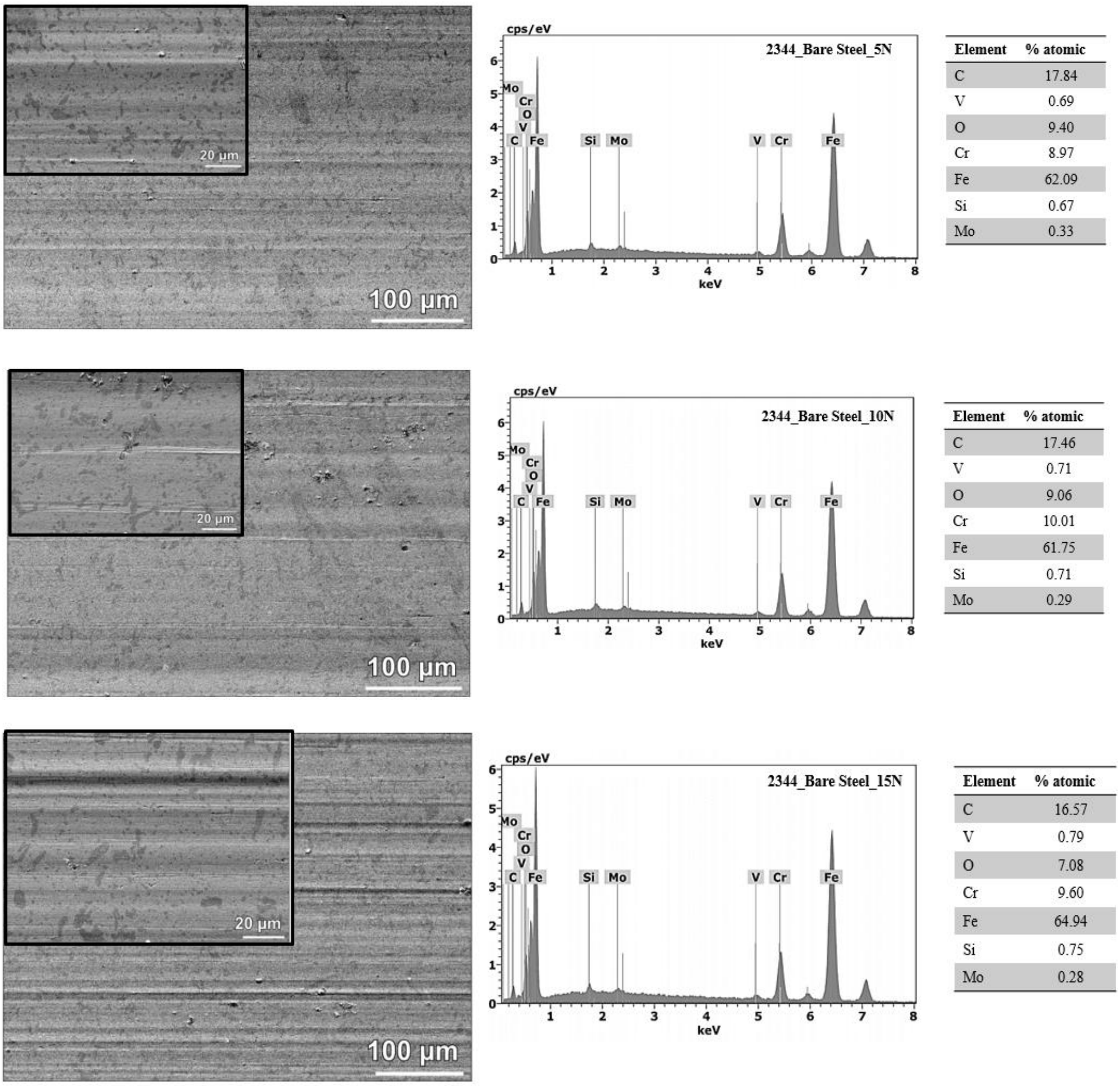

Figure 14. SEM/EDX analysis of the 2344 bare steel tested at 5N, 10N and 15N.

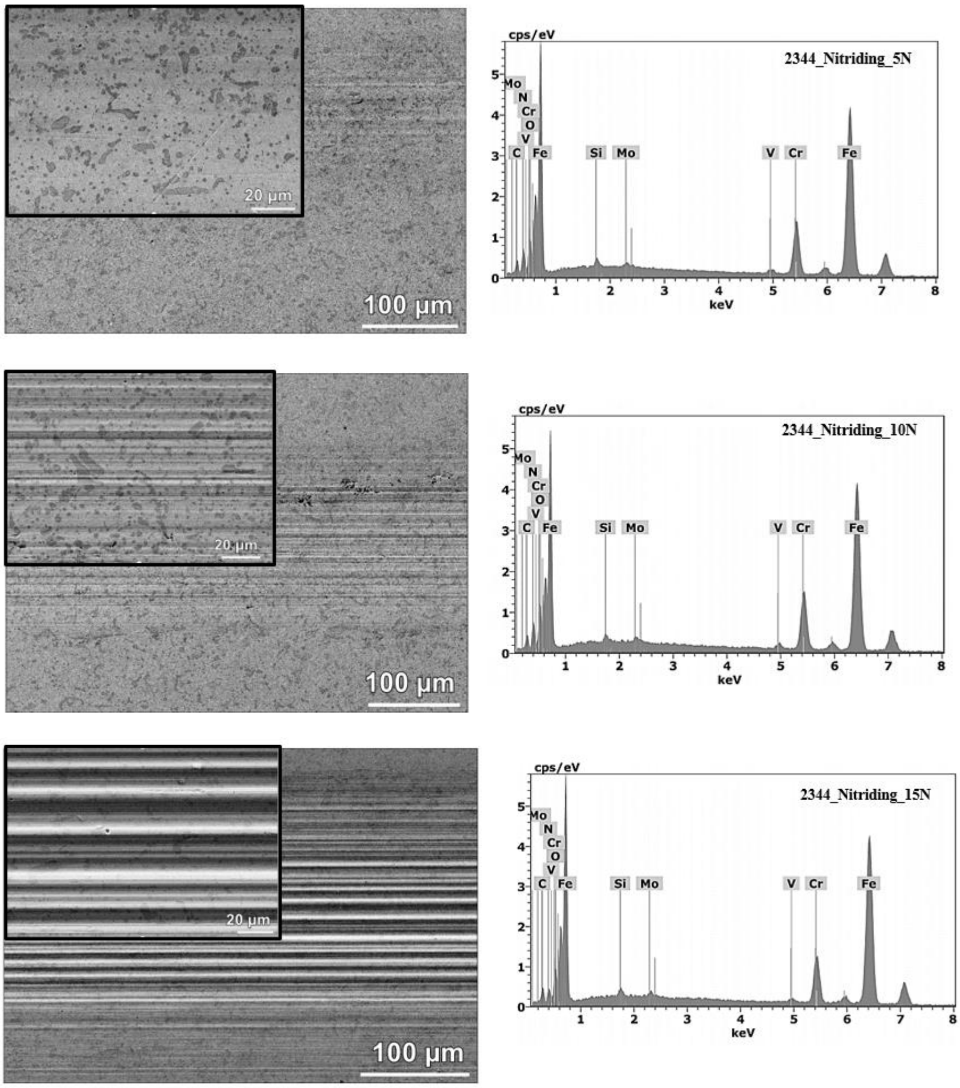

Element	% atomic
C	13.96
V	0.70
O	3.57
Cr	9.41
Fe	56.87
Si	0.06
Mo	0.06
N	14.37

Element	% atomic
C	13.19
V	0.74
O	6.36
Cr	9.71
Fe	53.90
Si	0.71
Mo	0.37
N	15.01

Element	% atomic
C	16.29
V	0.64
O	4.30
Cr	8.74
Fe	60.57
Si	0.66
Mo	0.28
N	8.52

Figure 15. SEM/EDX analysis of the 2344 nitrided steel tested at 5N, 10N and 15N.

2344 nitrided sample's SEM/EDX results were shown in Figure 15. When the SEM/EDX results of nitrided samples are examined, an expected increase in N percentage due to the nitriding process was observed. The higher level of Fe was detected with the load increase and the nitration layer decrease [16].

4. CONCLUSIONS

The mechanical and wear behavior of DIN 1.2344 hot-work tool steel, frequently used in the production area, is a significant research issue. The present study was performed to investigate the wear behavior of nitrided DIN 1.2344 hot work steel. The diffusion layers have been created as a result of the gas nitriding process in ammonia. Microscopic examinations exhibit that the microstructure varies from the surface to the core. The compound layer, diffusion zone, and core are illustrated in the optic microscope image of nitrided 2344 steel. The thickness of the diffusion zone was measured to be about 77 μm. The friction coefficient of the nitrided steel and non-nitrided 2344 steel increased in the early step of the wear tests. However, the friction coefficients of non-nitrided 2344 steel were higher than nitrided 2344 steel under all contact pressure. Wear scars analysis results indicated that the wear rate increased with a higher load at a constant sliding distance for both samples. The EDX analysis of nitride sample showed nitride precipitates exist within the grains and at the grain boundaries. Furthermore, Cr which is the base alloying element in DIN 2344 steel, has a comparatively intense chemical bond with nitrogen through the nitriding process. The consequence of the AFM analysis introduced that the abrasive wear scar depths of the nitrided sample were lower at 5N whereas similar depths were observed for at 10N and 15N. Herewith the wear resistance of steel was substantially advanced by the gas nitriding process. This work can also support the improvement and productive usage of hot work steel with these findings.

5. ACKNOWLEDGMENTS

The authors thank the support of the Scientific Research Projects Unit of Marmara University, Turkey for the funded project, Project no FEN-C-YLP-120619-0198 and Titanit Ultrahard PVD coatings company in Turkey.

REFERENCES

[1] Kostova, K.G., Uedaa, M., Lepienskyc, M., Soares Jr., P.C., Gomesa, G.F., Silvad, M.M., Reuther H. (2004). Surface Modification of Metal Alloys By Plasma Immersion Ion Implantation and Subsequent Plasma Nitriding. Surface and Coatings Technology, 186, 204–208.

[2] Castro, G., Fernández-Vicente, A., Cid, J. (2007). Influence of The Nitriding Time in The Wear Behavior of An AISI H13 Steel During A Crankshaft Forging Process. Wear, 263, 1375–1385.

[3] da Silva, L.L.G., Ueda, M., Nakazato, R. Z., (2007). Enhanced Corrosion Resistance of AISI H13 Steel Treated By Nitrogen Plasma Immersion Ion Implantation. Surface and Coatings Technology, 201, 8291–8294.

[4] Arif, A.F.M., Akhtar, S. S., Yilbas, B. S. (2010). Effect of ProcessVariables on Gas Nitriding of H13 Tool Steel With Controlled NitridingPotential. International Journal of Surface Science and Engineering, 4, 396–415.

[5] Rodrigo L.O. B., Heloise O. P., Vanessa S., Israel J.R. B., Silvia A.C. A., Fernando S. de S., Almir S., Carlos A. F., Cristiano G., (2010).Microstructure and Corrosion Behaviour of Pulsed Plasma-Nitrided AISI H13 Tool Steel. Corrosion Science, 52, 3133–3139.

[6] Yeh, S.-H., Chiu, L.-H., Chang, H. (2011). Effects of Gas Nitriding on the Mechanical and Corrosion Properties of SACM 645 Steel.Engineering, 3, 942–948.

[7] Rodríguez-Baracaldo, R., Benito, J. A., Puchi-Cabrera, E. S., Staia, M. H. (2007). High-Temperature Wear Resistance of (TiAl)N PVD Coatingon Untreated and Gas Nitrided AISI H13 Steel With Different Heat Treatments. Wear, 262, 380–389.

[8] Lampe, T., Eisenberg, S., Laudien, G. (1993). Compound LayerFormation During Plasma Nitriding and Plasma Nitrocarburising. Surface Engineering, 9, 69–76.

[9] Baranowska, J. (2010). Importance of Surface Activation for Nitrided Layer Formation on Austenitic Stainless Steel. Surface Engineering, 26,293–298.

[10] Birol, Y., Yuksel, B. (2012). Performance of Gas Nitrided and AlTiN Coated AISI H13 Hot Work Tool Steel in Aluminium Extrusion. Surface and Coatings Technology, 207, 461–466.

[11] Güven, Ş. Y., Delikanlı, K., Öncel, E. (2014). AISI 4140 ÇeliğineUygulanan İyon Nitrasyon Yüzey Sertleştirme İşleminin Yorulma Dayanımına Etkisi. SDU Teknik Bilimler Dergisi, 4, 29-39.

[12] Bayramoglu, M., Polat, H., Geren, N. (2008). Cost and Performance Evaluation of Different Surface Treated Dies for Hot Forging Process.Journal of Materials Processing Technology, 205, 394–403.

[13] Barrallier, L. (2015). Classical Nitriding of Heat Treatable Steel.Woodhead Publishing Limited, 393-412.

[14] Azadi, M., Rouhaghdam, A. S., Ahangarani, S., Mo, H. H. (2014). Mechanical Behavior of TiN / TiC Multilayer Coatings Fabricated By Plasma Assisted Chemical Vapor Deposition on AISI H13 Hot Work Tool Steel. Surface and Coatings Technology, 245, 156–166.

[15] Li, K. Y., Xiang, Z. D. (2010). Increasing Surface Hardness of Austenitic Stainless Steels By Pack Nitriding Process. Surface and Coatings Technology, 204, 2268–2272.

[16] Cui, X. H., Wang, S. Q., Wei, M. X., Yang, Z. R. (2011). Wear Characteristics and Mechanisms of H13 Steel with Various Tempered Structures. 20, 1055–1062.

[17] Arif, A.F.M., Akhtar, S. S., Yilbas, B. S. (2012). Influence of Multiple Nitriding on The Case Hardening of H13 Tool Steel: Experimental and Numerical Investigation. International Journal of Advanced Manufacturing Technology, 8, 57–70.

[18] Akhtar, S. S., Arif, A.F.M., Yilbas, B. S., Sheikh, A.K. (2010).Influence of Surface Preparation on the Kinetics of Controlled Gas-Nitrided AISI H13 Steels Used in Extrusion Dies, 19, 347–355.

[19] Greenwood, J. A. (1985). Formulas for Moderately Elliptical Hertzian Contacts, Journal of Tribology, 107, 501–504.

[20] Jordan, D., (2010). Controlling Compound (White) Layer Formation During Vacuum Gas Nitriding. Solar Atmospheres Inc., 1-20.

[21] Bahrami, A., Anijdan, S. H. M., Golozar, M. A., Shamanian, M., Varahram, N. (2005). Effects of Conventional Heat Treatment on Wear Resistance of AISI H13 Tool Steel. Wear, 258, 846–851.

[22] Jacobsen, S. D., Hinrichs, R., Aguzzoli, C., Figueroa, C. A., Baumvol, I. J. R., Vasconcellos, M. A. Z. (2016). Influence of Current Density on Phase Formation and Tribological Behavior of Plasma Nitrided AISI H13 Steel. Surface and Coatings Technology, 286, 129–139.

[23] Gasem, Z. M. (2013). Cracking in A Multiple Gas-Nitrided H13 Aluminum Extrusion Mandrel. Engineering Failure Analysis Journal, 31,68–75.

[24] Yang, K., Shi, X., Zhai, W., Mahmoud Ibrahim, A. M. (2015). WearRate of A Tial Matrix Composite Containing 10 Wt% Ag Predicted Using The Newton Interpolation Method. RSC Advances, 5, 67102-67114.

[25] Telasang, G., Dutta Majumdar, J., Padmanabham, G., Manna, I. (2015). Wear and Corrosion Behavior Laser Surface Engineered AISI H13 Hot Working Tool Steel. Surface and Coatings Technology 261, 69–78.

[26] Jeong, B. Y., Kim, M. H. (2001). Effects of Pulse Frequency and Temperature on The Nitride Layer and Surface Characteristics of Plasma Nitrided Stainless Steel. Surface and Coatings Technology, 137, 249–254.

[27] Fernandes, F. A. P., Heck, S. C., Picone, C. A., & Casteletti, L. C. (2020). On the wear and corrosion of plasma nitrided AISI H13. Surface and Coatings Technology, 381, 125216.

[28] Miyamoto, J., Abraha, P. (2019). The effect of plasma nitriding treatment time on the tribological properties of the AISI H13 tool steel.Surface and Coatings Technology, 375, 15–21.